DESIGN FOR MASS CUSTOMIZATION USING ADDITIVE MANUFACTURE: CASE-STUDY OF A BALLOON-POWERED CAR

Chen, Tian; Fritz, Stöckli; Shea, Kristina
Swiss Federal Institute of Technology in Zurich, Switzerland

Abstract

Additive Manufacturing offers unique advantages to produce customized designs. This paper demonstrates the capability for mass customization using Additive Manufacture through a case-study of a balloon powered car developed for a course. Two components of the assembly, the body and wheels are individualized by each student. To reduce the design-print iterations to a maximum of one while maintaining success rate of the fabricated parts, nine AM process constraints are determined through systematic physical tests. These are minimum dimensions, feature spacing and angles, and press fit tolerances and minimum overhang angle for self-supporting fabrication. A total of 2300 unique designs are created by the students and fabricated with Fused Deposition Modeling (FDM) using uPrint SE Plus. All function as intended with the exception of one set of wheels and many car bodies that omitted the press fit joint from the first iteration. No car bodies failed from the second iteration or due fabrication limitations. This demonstrates the effectiveness of the AM constraints determined and their upfront use in design to reduce design-print iteration rather than as a post-process.

Keywords: Computer aided design (CAD), Additive Manufacturing process characterization, design for additive manufacturing, mass customization

Contact:
Tian Chen
Swiss Federal Institute of Technology in Zurich
Engineering Design and Computing Laboratory, D-MAVT
Switzerland
ttc@ethz.ch

Please cite this paper as:
Surnames, Initials: *Title of paper*. In: Proceedings of the 20th International Conference on Engineering Design (ICED15), Vol. nn: Title of Volume, Milan, Italy, 27.-30.07.2015

1 INTRODUCTION

Driven by increasing interest in industry and the expiry of key patents, the overall cost of additive manufacturing (AM) technologies has decreased drastically over the past decade. At the same time, the variety of machines has significantly increased, making AM accessible for ever expanding applications (Hague, Campbell and Dickens, 2003). The technologies themselves have matured significantly and begun to offer new possibilities for designers to fabricate products that would not be feasible or cost-effective with conventional methods such as machining or injection molding. Doubrovski summarized potential applications of AM to part consolidation, weight reduction, functional customization, and aesthetics (Doubrovski, Verlinden and Geraedts, 2011) (Strömberg, 2010). In this research, we focus on functional customization of components that have dimensions in the meso, $i.e. 0.1 \rightarrow 10$ mm scale.

Despite the technological advancement, a large majority of 3D Printers in industry today are still used for the fabrication of prototypes (Wohlers Associates, Inc., 2014). In such usage, it is often not crucial to reduce printing time and material use and the accuracy level required is often less than for end-use parts. The general trend in AM is moving from prototyping applications towards small batch, end-use customized parts. Rather than re-using old designs fabricated with conventional means, to capitalize on the unique capabilities of AM, parts and products must be designed and optimized for AM in general and for the machines at one's disposal in particular.

This paper describes the testing of dimensional properties of Fused Deposition Modeling (FDM) machines with the goal to ensure printability of customized components and assemblies on the meso scale with little to no design iteration. Minimum dimensions, spacing and angles thus become critical design parameters at this scale. A set of constraints must be formulated and incorporated into the design process to ensure that novices with little knowledge of CAD and AM are able to design artifacts that can be fabricated as intended.

The design of a balloon propelled model car as part of a first semester Bachelor course exercise is used to demonstrate the process of incorporating tested Design for Additive Manufacturing (DfAM) constraints in a mass customization design exercise. Section 3 describes the exercise in detail. In summary, it requires each participant (473 in total) to model in CAD a model car assembly consisting of five unique parts, of which the wheel and body are to be customized. To minimize the number of design iterations to zero for the wheels and one for the body, a set of DfAM fabrication constraints specific to the 10 uPrint SE Plus FDM machines used are determined through systematic testing. Section 4 details the procedure and results of the printing experiments. Section 5 shows the resulting customized model car designs and discusses the implication of imposing DfAM constraints. The paper concludes with a brief discussion of the project and future work. A detailed account of the educational study of this exercise is presented in Chen et al. (2015).

2 BACKGROUND

2.1 FDM - Dimensional and mechanical properties of 3d printed components

FDM is an AM technology where two coils of thermoplastics are fed into separate printing nozzles that heat the materials past their glass transition temperature at the moment of extrusion. The extruded material hardens instantly and forms a base for further material to be deposited. The advantages of FDM include the ability to produce functional, plastic parts using a robust and cost-effective process that can be operated with little knowledge of AM, thus making it a good choice for educational use in mechanical engineering.

Mechanical and dimensional properties of the FDM process are actively investigated. Montero (2001) characterized FDM ABS plastic using designed experiments and compared the results with injection molded counterparts. The variables tested were raster orientation, air gap, bead width, color and model temperature. He concluded that the typical tensile strength from FDM ranges from 65 to 72 percent of injection molding. Too (2002) investigated the controllability and reproducibility of porosity and 3D microstructure. The parameters studied were raster gap, pore diameter, and strength. It was found that the porosity pore diameter and compressive strength depend principally on the raster gap size. FDM machines from Stratasys were used with ABS P400 as the build material in both of the above studies. Both studies focused primarily on the mechanical properties as a result of printability and did not address the dimensional aspects.

Meisel and Williams (2014) studied the Polyjet material jetting process and determine minimum printable feature sizes for fabrication and water-jet support material removal, and the overhang angle at which printed parts become self-supporting. Their test specimens follow from Moylan's standardized test artifact for AM (2012). Dimitrov (2006) investigated the achievable dimensional and geometric accuracy of inkjet 3D printing by printing two benchmark specimens. The factors tested were material used, nominal dimensions, build orientation, geometric features and topology, wall thickness, post treatment procedures, and infiltrating agent. The first, second, and third factors had the most influence on the resulting components. It was found that geometric accuracy is sufficient for small parts (i.e. 2 mm), though the summation of errors in larger parts may result in deviations too large for critical applications, i.e. assembly success depends on operator skills. The work in this paper uses a similar testing method and variables as Meisel and Dimitrov for FDM, and also considers fabrication optimization and press fit connection tolerance testing.

2.2 Mass customization with 3d printing

Mass customization focuses on generating variety from a base design or template to satisfy the need for personalization, and on minimizing cost and lead-time necessary to accomplish this (Williams and Mistree, 2006). The first objective is achieved in this exercise though modularizing the design and providing a base template that primarily addresses geometry of the connections. One achieves the second objective by leveraging the unique ability of AM to maintain a linear cost curve irrespective of the product being fabricated, i.e. the cost of tooling or mold-making is eliminated. Lastly, to ensure functionality, a set of DfAM constraints are provided to the designers to reduce iteration, especially considering a lack of experience with AM.

Examples of mass customization using 3D printing exist in specific niche industries. Shapeways.com (2012) provides an online 3D printing service for laymen and designers. To ensure printability, it supplies users with material dependent dimensional constraints including minimum wall thickness, wire dimension, embossed and engraved detail, escape holes, and clearance. The constraints are supplied primarily for ease of support material removal without damaging built parts. Many design guidelines for each material are given as a checklist and other constraints are manually checked on a model-by-model basis. With constrained mass customization, Invisalign fabricates a series of dental bracing molds that are customized to each patient's current and desired alignment (Inside 3DP, 2014). However, the variations in dimensions and spacing of the molds are minimal, therefore the process is heavily optimized.

2.3 Educational values

While the effectiveness of this exercise is outside the scope of this paper, numerous evidences suggest that mass customization, physical design iteration, and the use of AM contributes to improving student ability in the targeted areas. Williams and Mistree (2006) discusses incorporating mass customization in a Graduate Engineering Design Course, and concludes that it contributes to the internalization of course content. Sass presents a design methodology called Digital Design Fabrication (DDF) where CAD and AM are integrated into one process and presented several physical artifacts demonstrating its effectiveness (2006). Success is found by incorporating AM in design education as whole by Moeck et al. (2014) where comprehension and retention measures nearly doubles when compared with the control group.

3 PROJECT CHALLENGE

3.1 Problem statement

The goal is to develop an exercise to instruct students in 3D CAD modeling and assembly and to instill in students an understanding of virtual-physical design interaction. To that end, students are asked to design and model a mechanical device with a given CAD software package. Each design is then fabricated with AM and given back to the students. Based on this first iteration, students have the opportunity to re-design one part and have the second iteration fabricated as well. With a class size of approximately 473 students, the exercise is designed to achieve these goals:

- Produce designs that can be fabricated as intended and modeled with no or one iteration
- Provide sufficient freedom (overall dimensions and volume) for individual customization

- Minimize material use (both build and support material)
- Limit duration of fabrication to five working days with 10 uPrint SE Plus
- Minimize labor and cost during the pre- and post-processing stage
- The design example must be an assembly with the concept of tolerances incorporated

3.2 Description of the balloon powered car

The above requirements shaped the design that is developed for the exercise. Among different ideas explored, a model car is chosen. The constraint that the example must be an assembly with joints limits the idea space, but also creates an opportunity for the printing process. The car is decomposed into five unique components and nine components in total including four wheels, two axles, one chassis, one back, and one body. The body and the wheels are designed to be customizable by the students. For propulsion, a balloon is fixed to a cylindrical mount at the back of the car (Figure 1).

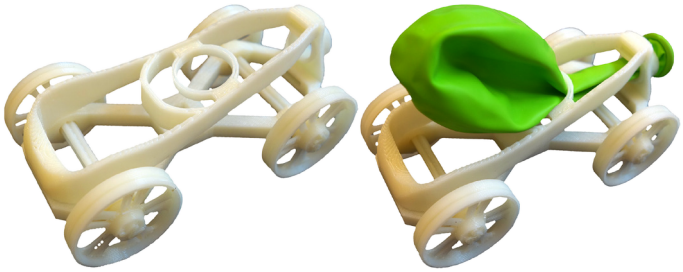

Figure 1. Balloon powered model car (L), and with the balloon propulsion (R)

3.3 Constraints and guidelines

In addition to the guidelines formulated in the next section, participants are provided with constraints for the design of the wheel and the body. For the wheel, a template including a predefined hub and rim and a solid spoke ($t = 1.0$ mm) is given to the participants with the intention of spoke customization (Figure 2). No iteration is allowed in the wheel design and printing. The body offers considerably more design freedom. A bounding box is provided to the participants with the press fit joints included. The participants can freely design the space within the bounding box with the constraint that the solid volume must be less than 5 cm^3, and that the design must connect to the two joints and be continuous and manifold. A single iteration is offered as an option to the participants.

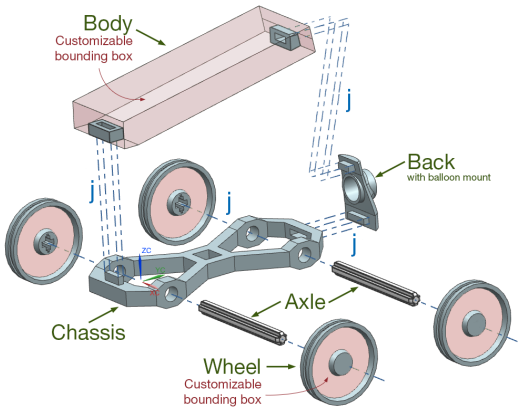

Figure 2. Assembly of the model car with wheel and body customization templates

3.4 Volume decomposition and press fit tolerance

While the car design can conceivably be printed as a single part, it is not effective to do so during a small batch mass production where reducing model and support material usage becomes important to economic viability and meeting the printing time constraint. The standard decomposed components are also optimized for printing time. Further, decomposition allows for iterative design and printing of the customized wheels and body. Material is saved by making cutouts in the chassis and by modeling it as a shell instead of a solid. The bigger cutout in the chassis is sized so that the back, with the

balloon mount, can be printed inside it. The chassis is shaped like figure eight so that one wheel may be printed in between every two chasses.

4 FDM - CONSTRAINT FORMULATION THROUGH PHYSICAL TESTING

While 3D printing has been marketed as being capable of producing three-dimensional objects of any geometry (Lipson and Kurman, 2013), there exist certain limitations that may cause components to not print as intended, or worse, to fail either during printing or post-processing. While all 3D printers use the STL file format as input, it is processed differently through each 3d printer manufacturer's own proprietary software packages, i.e. converting an .stl file to G-code. While different software perform largely the same tasks, the geometry validation and the extent to which users may influence the outcome vary greatly. Therefore, the authors determine eight geometric constraints that must be followed during the design process. The second goal of these constraints is to reduce the amount of support material used. This is achieved by setting a minimum overhang angle so that the build material becomes self-supporting. This not only reduces the cost and time of printing, but also the post-processing time to remove support material.

While these parameters are relevant in most AM methods, the precise value of each must be calibrated for each process and machine model. In this paper, the printer tested is the uPrint SE Plus by Stratasys. ABSplus in the color ivory is used as the model material for all test specimens, and SR-30 soluble for the support material. This printer offers a build platform of 203 x 203 x 152 mm.

As FDM is a layer-based fabrication method, differences exist in both tolerance and mechanical properties between the print-head axis (vertical) and the plate plane (horizontal). These quantities are formulated as constraints in Table 1, and shown in Figure 3.

Table 1. List of formulated geometrical constraints

Constraints formulation
Range of valid dimensions in the horizontal direction ($w_{\min}$) and in the vertical direction ($h_{\min}$)
Minimum spacing in the horizontal direction (s_{h}), and the vertical direction (s_{v})
Minimum interior (α_{I}) and exterior angle (α_{E})
Minimum angle of overhang to eliminate support material (θ_{OH})
Required tolerances for press fit joints (t)

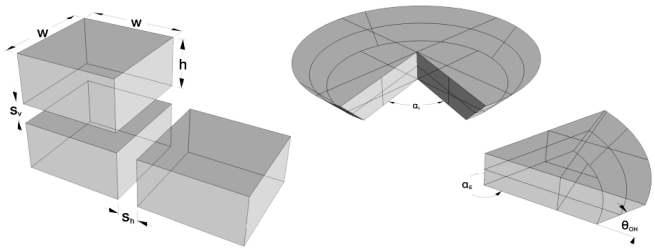

Figure 3. Part dimensions (w, h), spacing (s_v, s_h), and angles ($\alpha_I, \alpha_E, \theta_{OH}$) tested

CatalystEX version 4.4, UPrint's driver, provides several options for converting .stl to a sliced file. Unless specified otherwise, the options underlined in Table 2 are used to fabricate the test specimens.

Table 2. Options for converting geometry in CatalystEX v4.4

Layer resolution	0.254 mm	0.330 mm	
Model interior	Sparse - low density	Sparse - high density	Solid
Support fill	Basic	Smart	Surround

4.1 Description of Tests

4.1.1 Range of valid dimensions in the horizontal direction

A series of tokens are printed for each constraint, the dimensions reported follow the format $\mathrm{dim} = [\mathrm{min}\colon \mathrm{increment}\colon \mathrm{max}]$. The first aimed to determine the $w_{\min}$ of a design. To that end and to

assess the quality of the resulting components, rectangular prisms of increasing widths in the horizontal direction are printed. The width of the tokens equals to $w = [0.05{:}\ 0.05{:}\ 1.5]$.
The resulting widths are measured using a caliper with an error margin of ± 0.05 mm. It is observed that two contour lines are printed regardless of the thickness. With any widths below 1.0 mm (#01 to #20), the specimens are ~1.0 mm in width (Figure 4). This matches with the printer specification, which stated that the $w_{\min}$ of one contour (0.508 mm) is twice that of the layer thickness (0.254 mm). Beyond that threshold, the measured thickness is systematically larger than the design thickness by 0.05 mm. This could be attributed to measurement error.

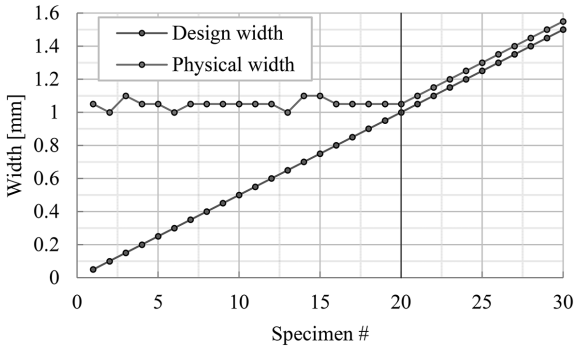

Figure 4. Test results - horizontal dimensions

Qualitatively, it is found that specimens between 1.15 to 1.25 mm (#22 to #24) exhibited significant reduction in lateral stiffness I_{zz}. This could be explained as follows. As demonstrated by Figure 5, when the width is sufficiently large (e.g. #30), the outlines are printed first, followed by the raster filling (indicated in red). With width at approximately 1.0 mm (#17), the two outlines touch and fuse into one cross section. In between the two extremes, however, the two outlines do not come into contact, but there is not sufficient room for the print head to deposit filling in the middle, resulting in an un-fused void. This issue causes the design in Figure 6 to fail as the hub along with the inner struts detaches with no resistance. Therefore, it is recommended to set the width $w_{\min} \geq 1.5$ mm.

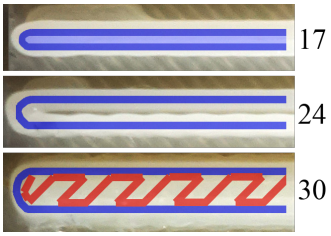

Figure 5. Gap between outlines

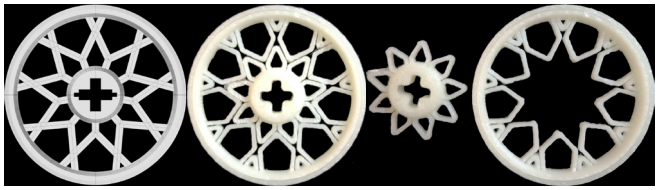

Figure 6. CAD (L) and failed result (R)

Additional specimens are printed at 30°, 45°, and 60° in orientation relative to the base plate to assess the effect of printing orientation to the print quality. It is found that they have no visible effect on either the quality or the dimensions. All four specimens are identical.

4.1.2 Minimum thickness in the vertical direction

A similar series of specimens are printed to determine the minimum vertical dimension. The layer height is set to 0.33 mm. The tested dimensions are $h = [0.05{:}\ 0.05{:}\ 3.0]$ mm. The tokens are printed onto two separate bases as the printer envelope is smaller than the length of one continuous piece.
As expected, the thicknesses increase directly proportional to the number of layers deposited on the model. The average thickness of one layer is 0.35 mm, which is within the printer specification. The resulting thicknesses are plotted in Figure 7, the staircase like increments corresponding to the layer thickness can be clearly observed. It is also evident that while both are systematically over-sized, specimen two is more accurate than specimen one. It is found that the number of layers deposited does not correlate directly to the thicknesses in the CAD design but rather to the relative thicknesses of the different tokens. In the first specimen (#1 to #26 or from 0.05 to 1.3 mm), tokens #1 to #5 are printed with single layers, and token #26 is printed with 6 layers. In the second specimen (#27 to #60, 1.35 to

3.00 mm), #27, which in design is 0.05 mm thicker than #26, is printed with only 5 layers, and thus corresponded better with the design.

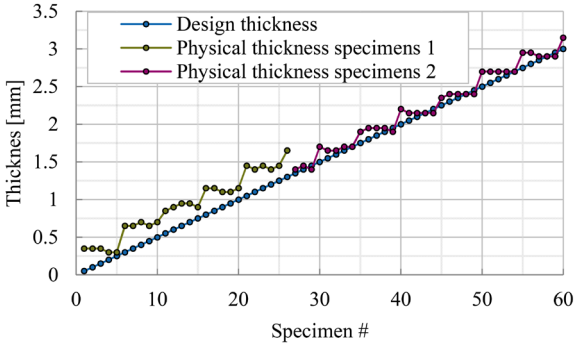

Figure 7. Design & physical thickness

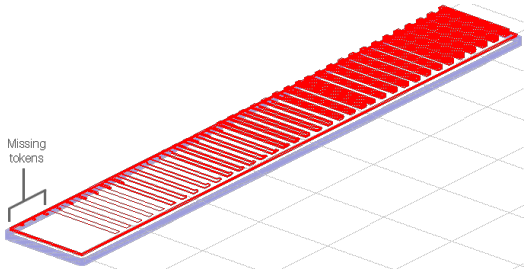

Figure 8. Thickness digital test

To test this observation further, a hypothetical continuous specimen (#1 to #60) is processed in CatalystEX. From the sliced file, it is found that token #1 to #3 would not be printed at all (Figure 8). This would explain the over-sizing of the tokens in the first specimen as CatalystEX tried to incorporate as much of the design as possible in the printout at the risk of misrepresentation.
The above suggests there would not be a definitive minimum. However, one is advised to keep the minimum layer to two as the one layered tokens deforms plastically during post-processing. This translates to a minimum thickness of $h_{\min} \geq 0.66$ mm.

4.1.3 Minimum spacing in the horizontal and vertical direction

A series of identical tokens are printed with increasing spacing between each. The thickness of individual tokens is set to be sufficiently large to require raster filling (1.5 mm). The spacing equals to $s_{\mathrm{h}} = [0.05,\ 0.1,\ 0.3{:}\,0.2{:}\,2.9]$mm. The spacing between #01 and #03 is lost in the printing. The spacing between #03 to #05 are measured indirectly as the tips of the caliper is not small enough to fit. Remaining tokens match the design spacing (Figure 9). The minimal spacing is set at $s_{\mathrm{h}} = 0.3$ mm.
The vertical spacing resolution is tested with story-like specimens. The "floors" are set at a constant thickness, and the story heights varies between $s_{\mathrm{v}} = [0.1{:}\,0.1{:}\,2.5]$ mm. These 25 tokens are divided into five separate specimens to fit within the print envelope. Due to the additive manufacturing process, "columns" must be added to support the upper "floors". The rest of the inter-storey void is filled with support material during printing, dissolved in post-processing, and then measured.

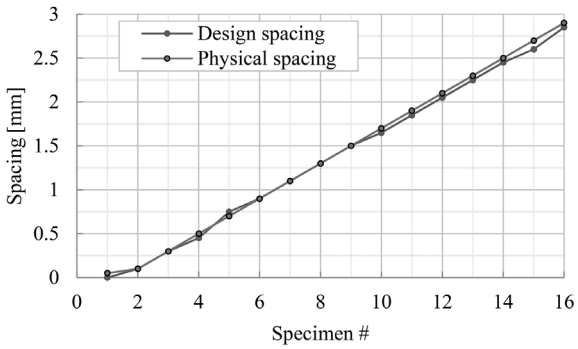

Figure 9. Horizontal spacing

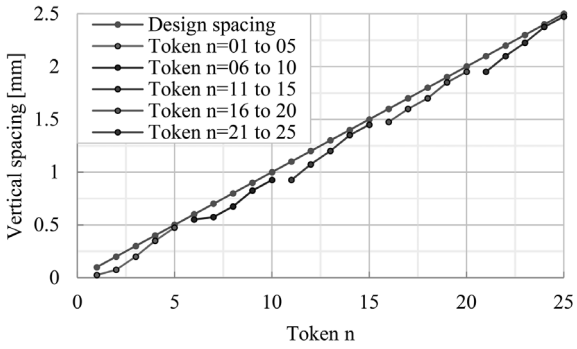

Figure 10. Vertical spacing

The results in Figure 10 show that the largest token within a specimen differ less than the specified 0.1 mm from the smallest token of the next specimen. These differences are compensated by the other tokens within the same specimen that had slightly larger spacing. Qualitatively, one of the two spacing in token $s_{\mathrm{v}} = 0.1$ mm fused with the floor, thus the minimum spacing is set at $s_{\mathrm{v}} \geq 0.2$ mm.

4.1.4 Minimum interior and exterior angles

As designs become more intricate, the angular features may become increasingly acute. To test the minimum printable angle, triangular wedges on a solid cylindrical surface are printed. The angles tests

are $\alpha = [5.1: 0.2: 12.9]°$. A complementary specimen containing the spaces in between the wedges are extruded and printed as well. The resulting specimens are shown in Figure 11 and Figure 12.

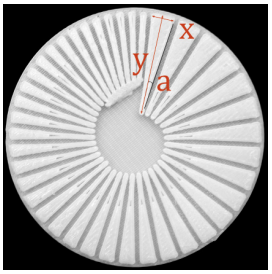

Figure 11. Wedges of varying angles

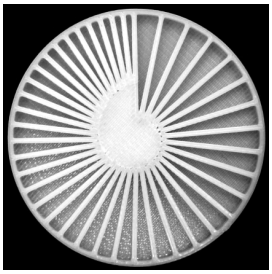

Figure 12. Wedges of varying spacing

The angles are measured indirectly by measuring the opposite (x) and the adjacent (y) lengths of each wedge using the caliper. From the resulting measurement (Figure 13 and Figure 14), it can be seen while these two specimens are printed separately, the smaller angles (#1 to 20) resulted in accurate angles and oversized spacing, and vice versa.

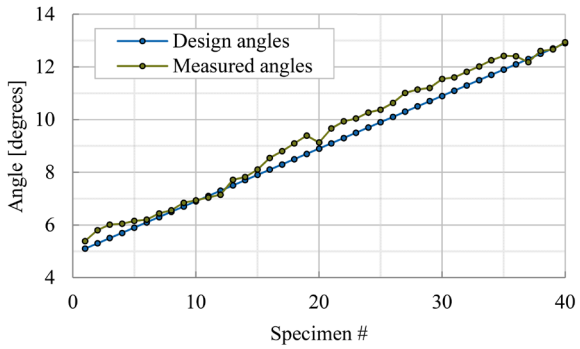

Figure 13. Wedge Spec. in Figure 11

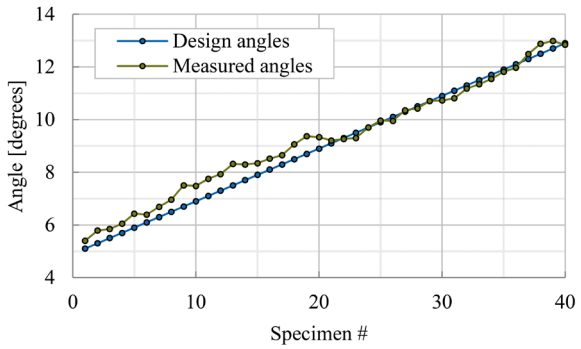

Figure 14. Spacing Spec. in Figure 12

Qualitatively, three observations can be made. 1) wedges 1 to 8 resulted in fused tips, making them defective. 2), all wedges have a gap near the tip, these gaps are caused by a similar phenomenon shown in Figure 5; there is insufficient space for the fill material. As the angle increases, the size of the gaps decreased as expected. 3), the tip of wedges are not sharp as in CAD due to the material deposition process. This defect is less pronounced with decreasing acuteness as well.
It is expected that these wedges would fail at the gap location under load. Therefore, while the absolute limit for acuteness may be set at $\alpha \geq 6.5°$, one should keep the acuteness above $\alpha \geq 10.0°$ to minimize the gap distance. For exterior angles, no degradation of quality is observed.

4.1.5 Angle of overhang to eliminate support material

As physical objects are subjected to gravity in the way that CAD designs are not, material must be deposited onto support material that may be removed after fabrication. The location and size of this support material is calculated automatically by the proprietary software to ensure that the component does not collapse during printing. Unfortunately, however, as in Catalyst EX, the designer cannot influence how the support material is distributed beyond three simple choices (Basic, Smart, and Covered), where "basic" covers all volume underneath the design with support material, "covered" envelopes the sides in addition to below, and "smart" takes the intermediate approach in order to conserve support material. With these options, it is impossible to force the printer to fabricate something that may collapse. Therefore, this overhang test is done with trial-and-error. It is found that with an $\theta_{\mathrm{OH}} \geq 45°$, no support material is needed for void above base plate, support, or build material.

4.1.6 Required tolerances for press fit joints

Press fit connections are used for assembly to eliminate separate connectors. Horizontal t_{H}, and vertical tolerance t_{V} are investigated as part of the design process. $t_{\mathrm{H}} = 0.1$ mm and $t_{\mathrm{H}} = 0.0$ mm is found to work well for a tight press fit parallel to the printing layers.

4.2 Summary of design constraints

Table 3. Summary of the resulting constraints

Dimensions	Range of validity	Comments
Range of invalid dimensions in the horizontal direction	$w \geq 1.5$ mm	1.0 mm if no load
Minimum thickness in the vertical direction	$h \geq 0.66$ mm	Equivalent of two layers
Minimum spacing in the horizontal direction	$s_{\mathrm{h}} \geq 0.1$ mm	
Minimum spacing in the vertical direction	$s_{\mathrm{v}} \geq 0.2$ mm	
Minimum interior angle	$\alpha_{\mathrm{I}} \geq 10.0°$	
Minimum exterior angle	$\alpha_{\mathrm{E}} \geq 0.0°$	No restriction
Angle of overhang to eliminate support material	$\theta_{\mathrm{OH}} \geq 45°$	For $t_{\mathrm{Layer}} = 0.0254$
Horizontal tolerance of press fit joints	$t_{\mathrm{H}} = 0.1$ mm	Resulting in a tight fit
Vertical tolerance of press fit joints	$t_{\mathrm{H}} = 0.0$ mm	

5 RESULTS OF CAR CUSTOMIZATION

473 students are given templates for the car wheels and body as shown in Figure 2 as well as for the wheel design the first six constraints in Table 3. The tolerance constraints determined are used in the design of the car assembly and templates. The overhang constraint is only used in this example to define a groove in the wheel that is part of the wheel template. Students are asked to design and model customized wheels without iteration and a car body using one iteration. Of the resulting unique solutions (413 wheel designs, and 421 body designs), samples are found in Figure 15. All second iteration bodies and all but one wheel printed successfully; one wheel failed due to human error. Many first iteration bodies failed due to the press fit joint being omitted by participants.

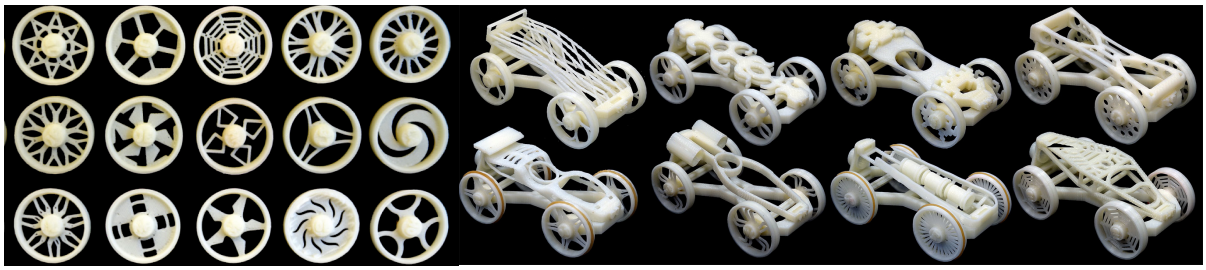

Figure 15. Selection of participant designed wheels (L) and model cars (R)

6 DISCUSSION

The resulting customized designs demonstrate the success of combining mass customization of an assembly with AM where customization of selected individual parts is carried out using a set of DfAM constraints. Unlike other methods, AM enables mass customization by laymen with little knowledge of the fabrication processes if sufficient DfAM guidelines and constraints are given. With the constraints determined through experiments targeted at this application, novice designers, i.e. first year students, could successfully design printable parts with zero and one iteration and with limited knowledge of FDM. From the variations in designs, it is hypothesized that the constraints does not limit the design space or their creativity. Further information on the academic study is provided in Chen et al. (2015). Based on the large pool of wheel and body designs printed, future work includes refining the set of DfAM constraints, especially related to more complex, 3D designs like the car body, and generalizing them beyond this example given so as to improve print quality while allowing design freedom. The constraints can also be used in generative design methods to automatically generate wheel and body design variants.

7 CONCLUSIONS

Through the example of a model car assembly, this paper demonstrates the applicability of constrained mass customization using 3D printers, namely FDM-based UPrint SE Plus. To guarantee successful fabrication with minimal design-print iteration, a series of nine fabrication constraints are determined

through physical tests. These are the min. dimensions, min. feature spacing in the horizontal and vertical directions, min. interior and exterior angle, press fit tolerances in both directions and min. overhang angle for self-supporting fabrication. The first six constraints are given to the students for the design exercise of the customized wheels and car body whereas the others are used in the design of the car assembly itself. Approximately 2300 unique designs are fabricated and examined, and all function as intended with the exception of one set of wheels due to a human error and many first iteration car bodies that omitted the press fit joint. The fact that none failed to fabricate shows the effectiveness of the constraints determined from tests. Future work will expand on the DfAM constraints and guidelines to improve, e.g. print quality for the wide geometric variation seen in the body design, as well as to generalize them for use in generative design methods (Chen and Shea, 2015).

REFERENCES

Chen, T., Egan, P., Stöckli, F. and Shea, K. (2015) Studying The Impact Of Incorporating An Additive Manufacturing Based Design Exercise In A Large, First Year Technical Drawing And Cad Course, To appear: Proceedings of International Design & Engineering Technical Conferences and Computers & Information in Engineering Conference, Boston, Massachusetts, USA.

Chen, T. and Shea, K. (2015) Computational Design-to-Fabrication Using Spatial Grammars: Automatically Generating Printable Car Wheel Design Variants, To appear: Proceedings of the 20th International Conference on Engineering Design, Milan.

Dimitrov, D., van Wijck, W., Schreve, K. and de Beer, N. (2006) Investigating the achievable accuracy of three dimensional printing, Rapid Prototyping Journal, vol. 12, no. 1, pp. 42-52.

Doubrovski, Z., Verlinden, J.C. and Geraedts, J.M.P. (2011) Optimal design for additive manufacturing: Opportunities and challenges, Proceedings of the ASME Design Engineering Technical Conference, pp. 635-646.

General Electric (2014) Advanced Manufacturing is Reinventing the Way We Work, [Online], Available: http://www.ge.com/stories/advanced-manufacturing [05 Nov 2014].

Hague, R., Campbell, I. and Dickens, P. (2003) Implications on design of rapid manufacturing, Proceedings of the Institution of Mechanical Engineers, Part C: Journal of Mechanical Engineering Science, pp. 25-30.

Inside 3DP (2014) How 3D Printing is Creating Unique Products, [Online], Available: http://www.inside3dp.com/3d-printing-creating-unique-products/ [16 Nov 2014].

Lipson, H. and Kurman, M. (2013) Fabricated: The New World of 3D Printing, 1st edition, Wiley.

Meisel, N.A. and Williams, C.B. (2014) Design For Additive Manufacturing: An Investigation Of Key Manufacturing Considerations In Multi-Material Polyjet 3d Printing.

Moeck, P., Stone-Sundberg, J., Snyder, T.J. and Kaminsky, W. (2014) Enlivening 300 level general education classes on nanoscience and nanotechnology with 3D printed crystallographic models, Journal of Materials Education, vol. 36, pp. 77-96.

Molyan, S., Slotwinski, J., Cooke, A., Jurrens, K. and Donmez, M.A. (2012) Proposal for a Standardized Test Artifact for Additive Manufacturing Machines and Processes, Texas.

Montero, M., Roundy, S., Odell, D., Ahn, S.H. and Wright, P.K. (2001) Material Characterization of Fused Deposition Modeling(FDM) ABS by Designed Experiments.

Sass, L. (2006) Materialization design: the implications of rapid prototyping in digital design, Design Studies, vol. 27, pp. 325-355.

Shapeways (2012) Detailed Plastic Material Information, [Online], Available: http://www.shapeways.com/materials/detailed-plastic [26 Nov 2014].

Stratasys (2014) NASA's Human-Supporting Rover has FDM Parts, [Online], Available: http://www.stratasys.com/resources/case-studies/aerospace/nasa-mars-rover [05 Nov 2014].

Strömberg, N. (2010) An Efficient Tradeoff Approach for Topology Optimization With Manufacturing Constraints, Proceedings of the ASME 2010 International Design Engineering Technical Conferences and Computers and Information in Engineering Conference, Montreal, 1171-1179.

Too, M.H., Leong, K.F., Chua, C.K., Du, Z.H., Yang, S.F., Cheah, C.M. and & Ho, S.L. (2002) Investigation of 3D non-random porous structures by fused deposition modelling, The International Journal of Advanced Manufacturing Technology, vol. 19, no. 3, pp. 217-223.

Williams, C.B. and Mistree, F. (2006) Empowering Students to Learn how to Learn: Mass Customization of a Graduate Engineering Design Course, International Journal of Engineering Education, vol. 22, no. 6, pp. 1269-1280.

Wohlers Associates, Inc. (2014) Wohlers Report 3d: Printing and Additive Manufacturing State of the Industry, Colorado: TERRY T. WOHLERS.